Greenland Ice Sheet Contribution to 21st Century Sea Level Rise as Simulated by the Coupled CESM2.1-CISM2.1

Laura Muntjewerf[1], Michele Petrini[1], Miren Vizcaino[1], Carolina Ernani da Silva[1], Raymond Sellevold[1], Meike D. W. Scherrenberg[1], Katherine Thayer-Calder[2], Sarah L. Bradley[3], Jan T. M. Lenaerts[4], William H. Lipscomb[2], Marcus Lofverstrom[5],

[1]Department of Geoscience and Remote Sensing, Delft University of Technology, Delft, The Netherlands
[2]Climate and Global Dynamics Laboratory, National Center for Atmospheric Research, Boulder, CO, USA
[3]Department of Geography, The University of Sheffield, Sheffield, UK
[4]Department of Atmospheric and Oceanic Sciences, University of Colorado Boulder, Boulder, CO, USA
[5]Department of Geosciences, University of Arizona, Tucson, AZ, USA

Key Points:

- CESM2.1-CISM2.1 simulates relatively strong warming and weakening of meridional overturning circulation by 2100.
- The Greenland ice sheet contributes 23 mm by 2050, and 109 mm by 2100, to global mean sea level rise.
- The role of the northern basins becomes progressively important as surface runoff strongly increases over the second half of the century.

Corresponding author: L. Muntjewerf, `L.Muntjewerf@tudelft.nl`

Abstract

The Greenland Ice Sheet (GrIS) mass balance is examined with an Earth system/ice sheet model that interactively couples the GrIS to the land and atmosphere. The simulation runs from 1850 to 2100, with historical and SSP5-8.5 forcing. By mid-21st century, the cumulative contribution to global mean sea level rise (SLR) is 23 mm. Over the second half of the 21st century, the surface mass balance becomes negative in all drainage basins, and an additional 86 mm of SLR is contributed. The annual mean GrIS mass loss in the last two decades is 2.7 mm sea level equivalent (SLE) yr^{-1}. Strong decrease in SMB (3.1 mm SLE yr^{-1}) is counteracted by a reduction in ice discharge from thinning and retreat of outlet glaciers. The southern GrIS drainage basins contribute 73% of the mass loss by mid-century. This decreases to 55% by 2100, as surface runoff in the northern basins strongly increases.

Plain Language Summary

The Greenland Ice Sheet (GrIS) is a vast mass of ice that slowly moves under the force of gravity. It gains mass at the surface from snowfall, and it loses mass from glacier calve at the ocean front. These two processes used to be in balance. Now, recent observations have found an acceleration in the mass loss, meaning an acceleration in the GrIS contribution the global mean sea level rise. This acceleration is thought to result from human-induced global warming.

This study uses a global model that both calculates ice flow of the GrIS, as well as processes in the other Earth components: the atmosphere, ocean, land, and sea-ice. To have a present-day reference, the model is provided with forcing (most importantly: atmospheric greenhouse gas concentrations) for the historical period (1850-2014). Next, we provide the model with forcing for the remainder of the 21st century (2015-2100). For this, the high-end SSP5-8.5 scenario is used in order to examine in what ways the GrIS and the global Earth system respond to the "worst-case" scenario.

By 2050, the GrIS has lost an amount of mass that is equal to 23 mm of global mean sea level rise. Over the second half of the 21st century, the overall GrIS surface is not gaining net mass anymore due in increased melting conditions. In particular, the role of the dry north becomes progressively important as meltwater runoff strongly increase. By 2100, the GrIS contribution to sea level rise is 109 mm sea level equivalent.

1 Introduction

The Greenland Ice Sheet (GrIS) has been losing mass at an increasing rate over the past two decades (Shepherd et al., 2019), and has recently become a major contributor to global mean sea-level rise (Chen et al., 2017). The IPCC Fifth Assessment Report identified the polar ice sheets as one of the main sources of uncertainty in 21st century sea-level rise projections (Church et al., 2013). A recent expert assessment estimates the GrIS cumulative contribution by 2100 to be between 20 and 990 mm, with a median of 230 mm (Bamber et al., 2019). The ice sheet and climate modelling communities have recently joined efforts to advance our understanding of ice sheet mass loss, and to improve future projections. This has come together in the Ice Sheet Modelling Intercomparison Project for CMIP6 (ISMIP6; Nowicki et al. (2016)). Part of the uncertainty in current SLR estimates stems from insufficient understanding of the complex interactions between ice sheets and the broader Earth system. This highlights the importance of coupled Earth system/ice-sheet models. ISMIP6 therefore proposed for coupled Earth system/ice sheet models to simulate the GrIS response under two different forcing scenarios: a) 1% per year increase in CO_2 to 4x pre-industrial concentration; and b) the historical period 1850-2014, followed by the remainder of the 21st century under the high-end SSP5-8.5 scenario (Shared Socioeconomic Pathways; O'Neill et al. (2016)).

In this study, the Community Earth System Model version 2 (CESM2; Danabasoglu et al. (accepted pending minor revisions)) with an interactive GrIS (CESM2.1-CISM2.1, (Muntjewerf et al., in preparation)) is used to simulate the period 1850-2100 under historical and SSP5-8.5 forcing. This paper presents the 21st century projections of the global climate and the Greenland ice sheet response, as well as the projected GrIS contribution to global mean sea level rise. Section 2 describes the model, ice-sheet/Earth system coupling, and the experiment design. Section 3 presents the results, with four subsections on the climate and whole-GrIS mass change, the partition of mass change per drainage basin, the freshwater budget, and a comparison to standard CESM2.1 simulations without an interactive GrIS. Section 4 discusses the results in the context of earlier studies, and draws the main conclusions.

2 Method: Model Description and Experimental Set-Up

2.1 The Community Earth System Model (CESM2)

The Community Earth System Model version 2 (CESM2) (Danabasoglu et al., accepted pending minor revisions) is a comprehensive, fully coupled, Earth system model that is contributing simulations of past, present, and future climates to the Coupled Model Intercomparison Project phase 6 (CMIP6; Eyring et al. (2016)). CESM2 includes component models of the atmosphere (CAM6), land (CLM5), ocean (POP2), sea-ice (CICE5), river transport (MOSART), and land-ice (CISM2.1; Lipscomb et al. (2019)). The simulations described here were run with nominal 1-degree horizontal resolution in the atmosphere, land, ocean, and sea ice components. The ice sheet model was run on a 4-km limited-area grid, centered on Greenland.

2.2 Interactive Earth System/Ice-Sheet Coupling

CESM2.1-CISM2.1 supports a time-evolving Greenland ice sheet that is interactively coupled to other Earth system components (Muntjewerf et al., in preparation). The surface mass balance (SMB) is computed in CLM5 as the difference between annual snow accumulation and surface ablation, derived from the surface energy balance. The SMB is calculated on multiple elevation classes to more accurately account for subgrid-scale variations in elevation-driven surface climate and SMB (Fyke et al., 2011; Lipscomb et al., 2013; Sellevold et al., 2019). The SMB is then downscaled to the higher-resolution ice-sheet model grid, using a trilinear interpolation scheme that separately conserves the total ablated and accumulated mass.

Freshwater fluxes from the ice sheet to the ocean are the sum of surface runoff from CLM5, and basal melt water and ice discharge from CISM2. Liquid water is routed to the ocean where it is distributed over the upper 30 m (Sun et al., 2017). Solid water is spread diffusively in the ocean surface layer (maximum distance of 300 km from the coast), where it is melted instantaneously using energy from the global ocean surface.

Dynamic land units in CLM5 enable the transition from glaciated to non-glaciated land cover, consistent with the evolving ice sheet margin in CISM2. The ice sheet surface topography in CISM2 is used to recompute the fractional glacier coverage in CLM5, subsequently affecting the albedo, soil, and vegetation characteristics. Surface elevation and topographic roughness fields in CAM6 are updated every 10 years to incorporate changes in the ice sheet geometry into atmospheric flow calculations.

2.3 Experimental Set-Up

Two simulations are analyzed in this study: the historical simulation between 1850-2014, and its continuation to 2100 following the SSP5-8.5 scenario (Nowicki et al., 2016; O'Neill et al., 2016). The historical forcing is based on observations of greenhouse gas concentrations, stratospheric aerosol data (volcanoes), land use change, and solar insolation. The pre-industrial (1850 CE) CO_2 concentration is 287 ppmv (parts per million by volume), and increases to 397 ppmv in year 2014. Further details on the historical simulations can be found in Eyring et al. (2016).

For the 21st century we used the SSP5-8.5 CMIP6 scenario (O'Neill et al., 2016). This scenario starts in 2015 from the end of the historical period, and ends in year 2100 when the atmospheric CO_2 concentration is 1142 ppmv. This means that the CO_2 concentration increases by approximately 1% per year (see Fig. 1a and Fig S4). This emission and land-use scenario produces a total anthropogenic radiative forcing of 8.5 W m^{-2} relative to pre-industrial in the year 2100.

The historical simulation starts from the spun-up pre-industrial model state described in Lofverstrom et al. (in review). In this state, the GrIS is in near-equilibrium with the simulated pre-industrial climate of CESM2.1. The GrIS residual drift is about 0.03 mm SLE yr^{-1}. This quasi-spun-up GrIS state overestimates the present-day observed volume by 12%, and area by about 15%.

2.4 Basin-Scale Analysis

For the regional scale analysis, we use the six major Greenland drainage basins as defined in Rignot and Mouginot (2012). The basin separation is based on glacier types (marine-terminating versus land-terminating) as well as SMB regime (dry versus wet). In regions where the ice sheet extent is overestimated, drainage basins are extended to the ice sheet margin. Finally, based on the flow direction we extend each drainage basin from the CISM margin into the ocean to define six major ice-ocean sectors to compute the freshwater discharged to the ocean from each basin.

3 Results

The analysis is focused on three climatological periods: contemporary period (averaged over years 1995-2014) from the historical simulation, and mid-century (2031-2050) and end-of-century (2081-2100) from the SSP5-8.5 simulation.

3.1 Evolution of Global Climate and GrIS Mass Budget

The atmospheric CO2 concentration increases in the SSP5-8.5 scenario from 287 ppmv in 1850, to 397 ppmv in 2014, 566 ppmv in 2050, and 1142 ppmv in 2100 (Figure 1, Table S1). Global mean temperatures increase by 5.4 K in the last two decades of the 21^{st} century relative to the pre-industrial era (simulation analysed in Muntjewerf et al. (submitted)). With respect to the contemporary period (1995-2014), the global temperature increases by 1.4 K mid-century and 4.6 K by end-of-century. The Arctic amplification factor, defined as the ratio of temperature change north of 60°N and of the global mean, is 2.0 by mid-century, and 1.8 by end-of-century.

The North Atlantic Meridional Overturning Circulation (NAMOC; defined as the maximum of the overturning stream function north of 28N and below 500 m depth in the North Atlantic basin) remains relatively stable throughout the historical period, with a mean index of 24 Sv (blue line in Fig. 1b); the only exception is an anomalously stronger overturning circulation in the 1960s when the NAMOC strength increases by about 3 Sv. The overturning cell becomes progressively weaker throughout the 21^{st} century, and has collapsed (8.6 Sv) by the end of the century (Table S2). The importance of Greenland freshwater fluxes for weakening NAMOC is discussed in section 3.3. A comparison of the NAMOC evolution in CESM2.1-only simulations (i.e., not including an interactive GrIS) is made in section 3.4.

The climate warming results in a positive GrIS contribution to global mean SLR (Figure 1c). The rate of ice mass loss increases from the pre-industrial near-equilibrium (0.03 mm SLE yr^{-1}) to 0.08 mm SLE yr^{-1} during the contemporary period, 0.55 mm SLE yr^{-1} by mid-century, and 2.68 mm SLE yr^{-1} by the end of the century (Table S1). Global mean temperature change at the time of mass loss acceleration is approximately 2.7 K with respect to pre-industrial. The mass evolution is in broad agreement with that in the 1% to $4xCO_2$ simulations that are performed with CESM2.1-CISM2.1 and CESM2.1-only; the the processes leading to this acceleration are discussed in further detail in Muntjewerf et al. (submitted) and Sellevold and Vizcaino (submitted), respectively. At the end of the century, the GrIS area and volume have decreased by 3% and 1.2% relative to the pre-industrial ice sheet, corresponding to a global mean SLR of 109 mm.

The surface mass balance (SMB) is the main contributor to the GrIS mass budget change (Figure 1d, Table S1). By mid-century, the GrIS integrated SMB is still positive (350 Gt yr^{-1}), and approximately 200 Gt yr^{-1} less than for the contemporary period (564 Gt yr^{-1}). The GrIS integrated SMB becomes negative by year 2077 based on the long-term linear trend. The rate of expansion of ablation areas (areas with average SMB ¡ 0) accelerates with similar timing. By mid-century, the SMB is strongly reduced in southern Greenland (Figure S1). By the end of the century, ablation areas extend far inland around the entire ice sheet, including along the northern periphery. The northern margins later than the southern margins; by end-of-century, northern surface mass loss has intensified and the equilibrium line altitude (the altitude where SMB=0) is much higher. In the interior of the ice sheet, SMB moderately increases due to greater snowfall.

The ice sheet thickness changes in broad agreement with changes in the surface mass balance. Most of the thinning occurs in the south and/or below the 2000-m elevation contour (Figure S1,b-c), and the thickness increases in the ice sheet interior (Figure S1,e-f). Surface velocities increase throughout the 21$^{\mathrm{st}}$ century the intermediate areas between the high interior and the ice sheet margins (Figure S1,h-i) due to the increase in surface elevation gradients resulting from SMB-induced thinning at the margins. Conversely, surface velocities at the margin decrease because of ice thinning and marginal retreat. As a result, the ice discharge is reduced by 8% (45 Gt yr^{-1}) by mid-century, and by 33% (189 Gt yr^{-1}) by the end of the century compared to the contemporary period (Table S1 and Figure S2). This partially compensates the mass loss from reduced SMB (214 Gt yr^{-1} and 1129 Gt yr^{-1} in mid-century and end-of-century, respectively (Table S1). These simulations do not include explicit ocean forcing of marine-based ice, and therefore outlet glacier acceleration is not simulated (Joughin et al., 2012).

3.2 Sea Level Rise Contribution by Drainage Basin

This section presents the mid-century and end-of-century mass balance change for individual drainage basins, with the contemporary mass budget as reference (Figure S3).

By mid-century, The mean total GrIS mass budget decreases by 196 Gt yr^{-1} by mid-century (-196 Gt yr^{-1}) (Figure 2), as a result of an SMB decrease of 38% (215 Gt yr^{-1}) partially compensated by a reduction in ice discharge of about 8% (45 Gt yr^{-1}). The SMB in all six drainage basins decreases but remains positive (Figure S3). Basins with the largest SMB reductions are the SW (-66 Gt yr^{-1}) and SE (-80 Gt yr^{-1}), decreasing with 79% and 36% compared to their contemporary values, respectively. A relatively smaller mid-century decrease in SMB is simulated in the NE basin (29%, -32 Gt yr^{-1}). The SMB changes are smallest in the CW, NW and NO basins. Taken together, the change in mass loss in the northern basins (NO, NW, NE) represents about 26% of the total SMB reduction (-55 Gt yr^{-1}). The relative change in contribution of these three basins to total GrIS SLR is 25% by mid-century (-43 Gt yr^{-1}).

At the end of the century (right panel in Figure 2), the mean total mass budget of the GrIS is reduced by 935 Gt yr^{-1} compared to the contemporary budget, from a -1129 Gt yr^{-1} reduction in SMB, which is partially (17%) compensated by a 189 Gt yr^{-1} reduction in ice discharge. Similarly, the basal melting increases by 4 Gt yr^{-1} by the end of the century. This term, however, is small compared to the total mass loss, and is thus disregarded in the rest of this discussion.

The largest end-of-century decrease in the SMB and ice discharge is simulated in the SE basin (290 Gt yr^{-1} and 81 Gt yr^{-1}), but this basin is the second largest in the total Greenland contribution to SLR (right panel in Figure S3). The SW basin is the largest contributor to global mean SLR, because the ice discharge decreases less than in the SE. Further, the decrease in the SMB is relatively high in the NE basin (-203 Gt yr^{-1}) where it results in a total mass budget decrease of -172 Gt yr^{-1} (right panel in Figure 2). The NO and NW basins show similar values of decrease in SMB (-145 and -141 Gt yr^{-1}), that together with the NE contribute 43% of the total GrIS SMB decrease. The relative part of these three basins to total GrIS SLR contribution (for this period 2081-2100) is 45%.

3.3 Freshwater Fluxes

The change in total-GrIS freshwater fluxes is comparatively moderate by mid-century, with runoff increasing less than 200 Gt yr^{-1} (from 427 to 619 Gt yr^{-1}), and some decrease in the solid freshwater flux which consists primarily of ice discharge (from 481 to

430 Gt yr^{-1}) (Figure 3). By this time, the NAMOC index has already decreased by 6 Sv (Figure 1 and Figure S4), suggesting that freshwater fluxes from Greenland play a comparative minor role for weakening the NAMOC. A similar result is found for a 1% to four-times-CO_2 simulation with the coupled CESM2.1-CISM2.1 ((Muntjewerf et al., submitted); compare time series of freshwater fluxes there with Figure S4).

By end-of-century, runoff has more than tripled relative to the contemporary period (to 1445 Gt yr^{-1}) (Figure 3). The reduction in ice discharge (to 260 Gt yr^{-1}), however, results in a total freshwater flux that is only 1.5 times the contemporary flux. Per basin, the SW and SE regions contribute the largest volume to the total runoff during all periods. However, their contribution decreases relatively from 63% (267 Gt yr^{-1} on a GrIS total of 427 Gt yr^{-1}) in the contemporary period to 48% (696 Gt yr^{-1} on a GrIs total of 1445 Gt yr^{-1}) in the end-of-century period. This is due to an increasing contribution of the northern basins (NW, NE, and NO) from a relative large increase in runoff. They contribute 44% (642 Gt yr^{-1}) of the total-GrIS runoff by end-of-century, as opposed to 29% (129 Gt yr^{-1}) in the contemporary period.

During all periods, the SE region contributes the most in absolute terms to the GrIS ice discharge (Figure 3). Relative to the contemporary discharge, all basins have similar reductions by mid-century (around 10%), however by end-of-century the northern basins have the highest reductions (up to 73% for NO). This higher sensitivity is in agreement with the comparison of the evolution of seven major outlet glaciers from different basins in Muntjewerf et al. (submitted).

3.4 Comparison with CESM2 Simulations without Interactive Greenland Ice Sheet

Finally, we compare the SMB and NAMOC responses to the historical ensembles and a suite of scenario simulations that were conducted without an interactive GrIS (CESM2.1). This section does not consider total SLR contribution, as diagnoses of SLR from CESM2.1 would tend to be overestimated because of missing the negative feedback of ice discharge as described in sections 3.1 and 3.2. We consider 11 CESM2.1 ensemble members from the historical period, and the following scenario simulations between 2015-2100: SSP1-2.6 (2 members), SSP2-4.5 (3 members), SSP3-7.0 (2 members), and SSP5-8.5 (2 members), with the scenario details provided by O'Neill et al. (2016).

For the SMB, the CESM2.1 simulations show a lower contemporary SMB and a lower end-of-century SMB, and a higher SMB sensitivity to warming thatn CESM2.1-CISM2.1 (Figure 4 and Table S2). The reduction in SMB between the full historical mean [1850-2014] and the contemporary mean [1995-2014] is larger in CESM2.1 (-65 Gt yr^{-1}: from 455 to 390 Gt yr^{-1}) than in CESM2.1-CISM2.1 (-17 Gt yr^{-1}: from 588 to 571 Gt yr^{-1}). This difference in response is likely due to the area and volume overestimation of the spun-up GrIS (Lofverstrom et al., in review). The contemporary CESM2.1-CISM2.1 overestimates the SMB (Noël et al., 2018) and simulates higher interannual SMB variability than CESM2.1 (80 Gt yr^{-1} vs. 28 Gt yr^{-1}), whereas CESM2.1 simulates a realistic SMB (Noël et al., 2019).

For end of century under SSP5-8.5 forcing, the SMB is almost 400 Gt yr^{-1} lower for CESM2.1 compared with CESM2.1-CISM2.1 (-906 vs -511 Gt yr^{-1}). Part of the smaller SMB reduction in the CESM2.1-CISM2.1 run is likely because high-melt areas on the margin are removed dynamically, whereas they are allowed to remain in the non-evolving CESM2.1 simulation. This result is consistent with results of the CESM2.1 versus CESM2.1-CISM2.1 comparison for the idealised simulations of 1% per year CO_2 increase to 4x pre-industrial (Sellevold & Vizcaino, submitted; Muntjewerf et al., submitted). Regardless of these differences in the magnitude of the SMB response, the SMB evolution shows similar timing for both models. The CESM2.1-CISM2.1 response to SSP5-8.5 exceeds the CESM2.1 response to less extreme scenarios (e.g., SSP3-7.0).

The NAMOC index evolves in a similar fashion in both CESM2.1-CISM2.1 and CESM2.1 simulations (Figure 4 and Table S2). The peak of the NAMOC strength in the second half of the 20th century is simulated by both models.

4 Discussion and Conclusions

The projected GrIS contribution to SLR of 109 mm by 2100 is in general agreement with pre-AR5 multi-model results (Bindschadler et al., 2013) and the AR5 assessment (Church et al., 2013). The latter gives a likely range of 70 to 210 mm. Our projection also lies within the range of post-AR5 estimates from Fürst et al. (2015); Calov et al. (2018) and Golledge et al. (2019), which are of 102 mm [std.dev 32], 46-130 mm, and 112 mm, respectively. A lower estimate (58 mm) is given by Vizcaino et al. (2015) with a coupled Earth system/ice sheet model of coarse (3.75 degrees) resolution with energy-balance-based melt calculation. A higher range (140-330 mm) is estimated by Aschwanden et al. (2019) with an ice sheet model forced with spatially uniform warming.

The SSP5-8.5 scenario simulation relates to the idealized 1% simulation (Muntjewerf et al., submitted), because the atmospheric CO_2 concentration at the end of the SSP5-8.5 reaches the same value as the idealized simulation does in year 140: when quadrupled pre-industrial values are reached (see Table S1 and Figure S4). The last two decades of the SSP5-8.5 simulation and the two decades when reaching quadrupled atmospheric CO_2 (131-150) have a similar global mean temperature, GrIS ice discharge, and cumulative contribution to global mean SLR. The mass balance is lower in the SSP5-8.5 as a result of a more negative SMB, hence the SSP5-8.5 reaches a higher rate of GrIS contribution to global mean SLR. Finally, the NAMOC differs with a later start of the weakening, and more remaining overturning strength by the end of the 21$^{\text{st}}$ under SSP5-8.5 forcing.

The presented simulations have been one of the first with CESM2.1-CISM2.1 including an interactive Greenland ice sheet. In conclusion, the contribution to sea level rise is 23 mm by 2050, with an additional 85 mm by 2100 in the SSP5-8.5-scenario of the 21$^{\text{st}}$ century. Also, we have seen that the contribution from northern basins to sea level rise is minor by mid-century, but becomes of similar magnitude as the southern contribution by the end of the century.

Acknowledgments

CESM2 is an open source model, available at: http://www.cesm.ucar.edu/. The CESM project is supported primarily by the National Science Foundation (NSF). This material is based upon work supported by the National Center for Atmospheric Research, which is a major facility sponsored by the NSF under Cooperative Agreement No. 1852977. Computing and data storage resources, including the Cheyenne supercomputer (`doi: 10.5065/D6RX99HX`), were provided by the Computational and Information Systems Laboratory (CISL) at NCAR.

LM, MP, MV, and CES acknowledge funding from the European Research Council (grant no. ERC-StG-678145-CoupledIceClim). RS acknowledges funding from the Dutch Research Council (NWO) (grant no. xxx).

The World Climate Research Program (WGCM) Infrastructure Panel is the official CMIP document home: `https://www.wcrp-climate.org/wgcm-cmip`. The CMIP6 and ISMIP6 historical and SSP simulations simulations are freely available, and accessible via the Earth System Grid Federation (ESGF) data portals `https://esgf.llnl.gov/nodes.html`.

References

Aschwanden, A., Fahnestock, M. A., Truffer, M., Brinkerhoff, D. J., Hock, R., Khroulev, C., ... Khan, S. A. (2019). Contribution of the greenland ice sheet to sea level over the next millennium. *Science Advances*, *5*(6). Retrieved from `https://advances.sciencemag.org/content/5/6/eaav9396` doi: 10.1126/sciadv.aav9396

Bamber, J. L., Oppenheimer, M., Kopp, R. E., Aspinall, W. P., & Cooke, R. M. (2019). Ice sheet contributions to future sea-level rise from structured expert judgment. *Proceedings of the National Academy of Sciences*, *116*(23), 11195–11200. Retrieved from `https://www.pnas.org/content/116/23/11195` doi: 10.1073/pnas.1817205116

Bindschadler, R. A., Nowicki, S., Abe-Ouchi, A., Aschwanden, A., Choi, H., Fastook, J., ... et al. (2013). Ice-sheet model sensitivities to environmental forcing and their use in projecting future sea level (the searise project). *Journal of Glaciology*, *59*(214), 195–224. doi: 10.3189/2013JoG12J125

Calov, R., Beyer, S., Greve, R., Beckmann, J., Willeit, M., Kleiner, T., ... Ganopolski, A. (2018). Simulation of the future sea level contribution of greenland with a new glacial system model. *The Cryosphere*, *12*(10), 3097–3121. Retrieved from `https://www.the-cryosphere.net/12/3097/2018/` doi: 10.5194/tc-12-3097-2018

Chen, X., Zhang, X., Church, J. A., Watson, C. S., King, M. A., Monselesan, D., ... Harig, C. (2017). The increasing rate of global mean sea-level rise during 1993–2014. *Nature Climate Change*, *7*(7), 492–495. Retrieved from `https://doi.org/10.1038/nclimate3325` doi: 10.1038/nclimate3325

Church, J., Clark, P., Cazenave, A., Gregory, J., Jevrejeva, S., Levermann, A., ... Unnikrishnan, A. (2013). Sea level change [Book Section]. In T. Stocker et al. (Eds.), *Climate change 2013: The physical science basis. contribu-*

tion of working group i to the fifth assessment report of the intergovernmental panel on climate change (p. 1137â1216). Cambridge, United Kingdom and New York, NY, USA: Cambridge University Press. Retrieved from www.climatechange2013.org doi: 10.1017/CBO9781107415324.026

Danabasoglu, G., et al. (accepted pending minor revisions). The community earth system model version 2 (cesm2). *Journal of Advances in Modeling Earth Systems*.

Eyring, V., Bony, S., Meehl, G. A., Senior, C. A., Stevens, B., Stouffer, R. J., & Taylor, K. E. (2016). Overview of the coupled model intercomparison project phase 6 (cmip6) experimental design and organization. *Geoscientific Model Development*, *9*(5), 1937–1958. Retrieved from https://www.geosci-model-dev.net/9/1937/2016/ doi: 10.5194/gmd-9-1937-2016

Fürst, J. J., Goelzer, H., & Huybrechts, P. (2015). Ice-dynamic projections of the greenland ice sheet in response to atmospheric and oceanic warming. *The Cryosphere*, *9*(3), 1039–1062. Retrieved from https://www.the-cryosphere.net/9/1039/2015/ doi: 10.5194/tc-9-1039-2015

Fyke, J. G., Weaver, A. J., Pollard, D., Eby, M., Carter, L., & Mackintosh, A. (2011). A new coupled ice sheet/climate model: description and sensitivity to model physics under eemian, last glacial maximum, late holocene and modern climate conditions. *Geoscientific Model Development*, *4*(1), 117–136. Retrieved from http://www.geosci-model-dev.net/4/117/2011/ doi: 10.5194/gmd-4-117-2011

Golledge, N. R., Keller, E. D., Gomez, N., Naughten, K. A., Bernales, J., Trusel, L. D., & Edwards, T. L. (2019). Global environmental consequences of twenty-first-century ice-sheet melt. *Nature*, *566*(7742), 65–72. Retrieved from https://doi.org/10.1038/s41586-019-0889-9 doi: 10.1038/s41586-019-0889-9

Joughin, I., Alley, R. B., & Holland, D. M. (2012). Ice-sheet response to oceanic forcing. *Science*, *338*(6111), 1172–1176. Retrieved from http://science.sciencemag.org/content/338/6111/1172 doi: 10.1126/science.1226481

Lipscomb, W. H., Fyke, J. G., VizcaÃno, M., Sacks, W. J., Wolfe, J., Vertenstein, M., ... Lawrence, D. M. (2013). Implementation and initial evaluation of the glimmer community ice sheet model in the community earth system model.

Journal of Climate, *26*(19), 7352-7371. Retrieved from https://doi.org/10.1175/JCLI-D-12-00557.1 doi: 10.1175/JCLI-D-12-00557.1

Lipscomb, W. H., Price, S. F., Hoffman, M. J., Leguy, G. R., Bennett, A. R., Bradley, S. L., ... Worley, P. H. (2019). Description and evaluation of the community ice sheet model (cism) v2.1. *Geoscientific Model Development*, *12*(1), 387–424. Retrieved from https://www.geosci-model-dev.net/12/387/2019/ doi: 10.5194/gmd-12-387-2019

Lofverstrom, M., et al. (in review). Ice-sheet/climate spin-up between cesm2.1 and cism2.1. *Journal of Advances in Modeling Earth Systems*.

Muntjewerf, L., Sacks, W. J., Lofverstrom, M., Fyke, J., Lipscomb, W. H., Ernani da Silva, C., ... Lenaerts, J. T. M. (in preparation). Description and demonstration of the coupled community earth system model v2.1 - community ice sheet model v2.1 (cesm2.1-cism2.1). *Journal of Advances in Modeling Earth Systems*.

Muntjewerf, L., Sellevold, R., Vizcaino, M., Ernani da Silva, C., Petrini, M., Thayer-Calder, K., ... Sacks, W. J. (submitted). Accelerated greenland ice sheet mass loss under high greenhouse gas forcing as simulated by the coupled cesm2.1-cism2.1. *Journal of Advances in Modeling Earth Systems*.

Noël, B., van de Berg, W. J., van Wessem, J. M., van Meijgaard, E., van As, D., Lenaerts, J. T. M., ... van den Broeke, M. R. (2018). Modelling the climate and surface mass balance of polar ice sheets using racmo2 – part 1: Greenland (1958–2016). *The Cryosphere*, *12*(3), 811–831. Retrieved from https://www.the-cryosphere.net/12/811/2018/ doi: 10.5194/tc-12-811-2018

Noël, B., van Kampenhout, L., van de Berg, W. J., Lenaerts, J. T. M., Wouters, B., & van den Broeke, M. R. (2019). Brief communication: Cesm2 climate forcing (1950â“2014) yields realistic greenland ice sheet surface mass balance. *The Cryosphere Discussions*, *2019*, 1–17. Retrieved from https://www.the-cryosphere-discuss.net/tc-2019-209/ doi: 10.5194/tc-2019-209

Nowicki, S. M. J., Payne, A., Larour, E., Seroussi, H., Goelzer, H., Lipscomb, W., ... Shepherd, A. (2016). Ice sheet model intercomparison project (ismip6) contribution to cmip6. *Geoscientific Model Development*, *9*(12), 4521–4545. Retrieved from https://www.geosci-model-dev.net/9/4521/2016/ doi:

10.5194/gmd-9-4521-2016

O'Neill, B. C., Tebaldi, C., van Vuuren, D. P., Eyring, V., Friedlingstein, P., Hurtt, G., ... Sanderson, B. M. (2016). The scenario model intercomparison project (scenariomip) for cmip6. *Geoscientific Model Development*, *9*(9), 3461–3482. Retrieved from `https://www.geosci-model-dev.net/9/3461/2016/` doi: 10.5194/gmd-9-3461-2016

Rignot, E., & Mouginot, J. (2012). Ice flow in greenland for the international polar year 2008–2009. *Geophysical Research Letters*, *39*(11).

Sellevold, R., van Kampenhout, L., Lenaerts, J. T. M., Noël, B., Lipscomb, W. H., & Vizcaino, M. (2019). Surface mass balance downscaling through elevation classes in an earth system model: analysis, evaluation and impacts on the simulated climate. *The Cryosphere Discussions*, *2019*, 1–25. Retrieved from `https://www.the-cryosphere-discuss.net/tc-2019-122/` doi: 10.5194/tc-2019-122

Sellevold, R., & Vizcaino, M. (submitted). Global warming threshold and mechanisms for greenland ice sheet surface mass loss. *Journal of Advances in Modeling Earth Systems*.

Shepherd, A., Ivins, E., Rignot, E., Smith, B., van den Broeke, M., Velicogna, I., ... Team, T. I. (2019). Mass balance of the greenland ice sheet from 1992 to 2018. *Nature*. Retrieved from `https://doi.org/10.1038/s41586-019-1855-2` doi: 10.1038/s41586-019-1855-2

Sun, Q., Whitney, M. M., Bryan, F. O., & heng Tseng, Y. (2017). A box model for representing estuarine physical processes in earth system models. *Ocean Modelling*, *112*, 139 - 153. Retrieved from `http://www.sciencedirect.com/science/article/pii/S146350031730029X` doi: https://doi.org/10.1016/j.ocemod.2017.03.004

Vizcaino, M., Mikolajewicz, U., Ziemen, F., Rodehacke, C. B., Greve, R., & van den Broeke, M. R. (2015). Coupled simulations of greenland ice sheet and climate change up to a.d. 2300. *Geophysical Research Letters*, *42*(10), 3927-3935. Retrieved from `https://agupubs.onlinelibrary.wiley.com/doi/abs/10.1002/2014GL061142` doi: 10.1002/2014GL061142

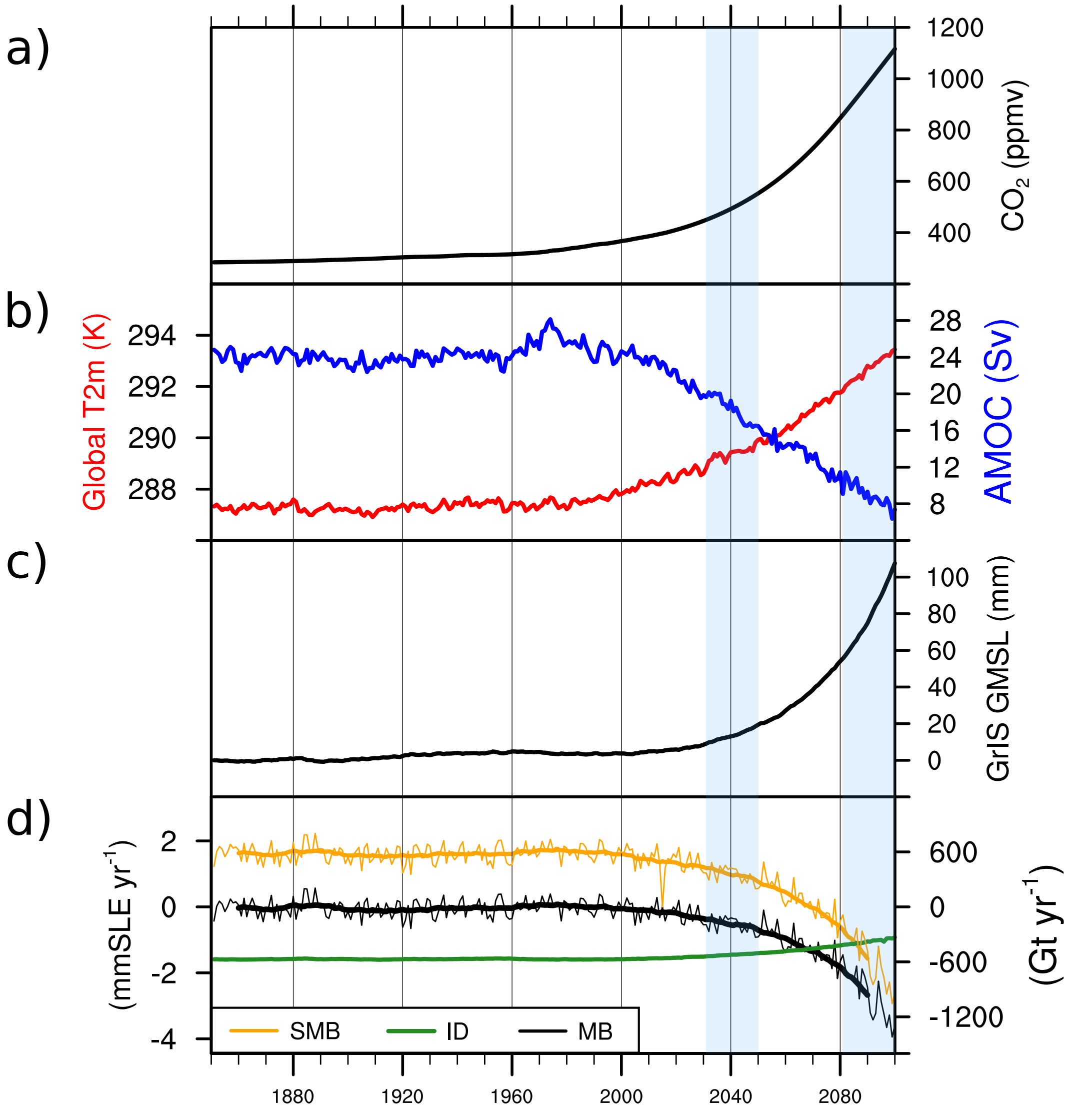

Figure 1. 1850-2100 evolution of (a) CO_2 forcing; (b) global mean temperature (K) and AMOC index (Sv); (c) cumulative sea level rise; and (d) Mass Balance (MB) contribution to global mean sea level rise with right axis: Gt yr^{-1}, left axis: mm yr^{-1}) and components of the mass budget (SMB, Ice Discharge). The shared areas in blue denote the mid-century (2031-2050, left), and end-of-century (2081-2100, right) periods.

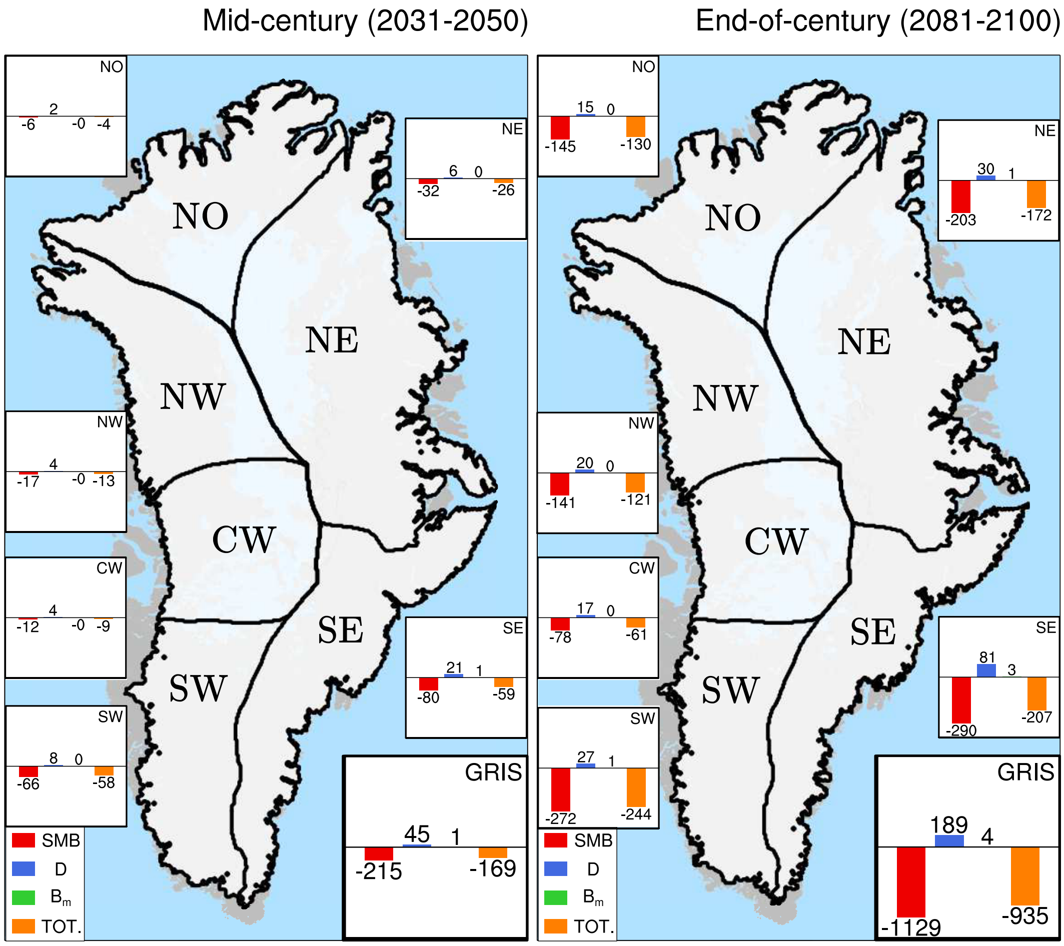

Figure 2. Change in mass budget (TOT) and components with respect to the contemporary budget (1995-2014) for mid-century (2031-2050, left), and end-of-century (2081-2100, right), in Gt yr^{-1}. TOT (Orange)=SMB (Red) + D(Discharge) + Bm (Basal Melt). Note that discharge is defined as negative.

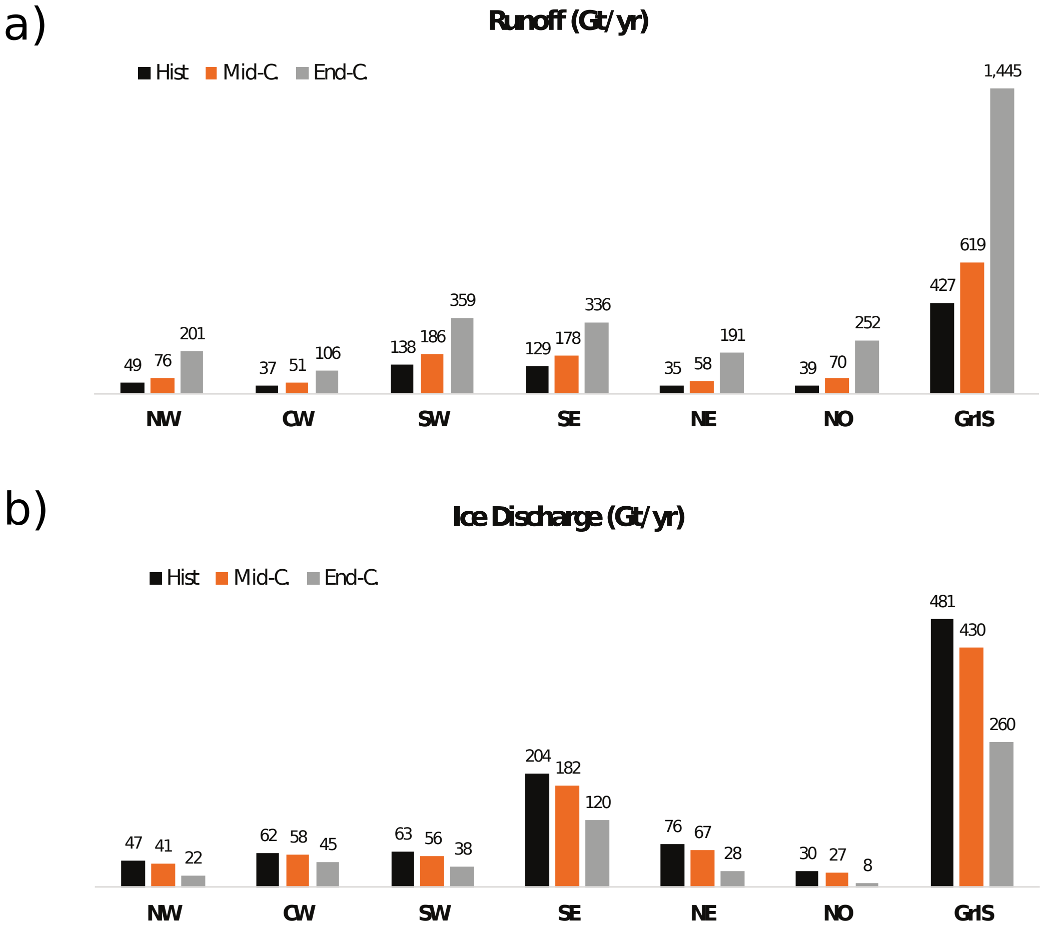

Figure 3. Freshwater flux (Gt yr^{-1}) from (a) Greenland runoff; (b) ice discharge (Gt yr^{-1}) per basin for the contemporary, mid-century and end-of-century periods.

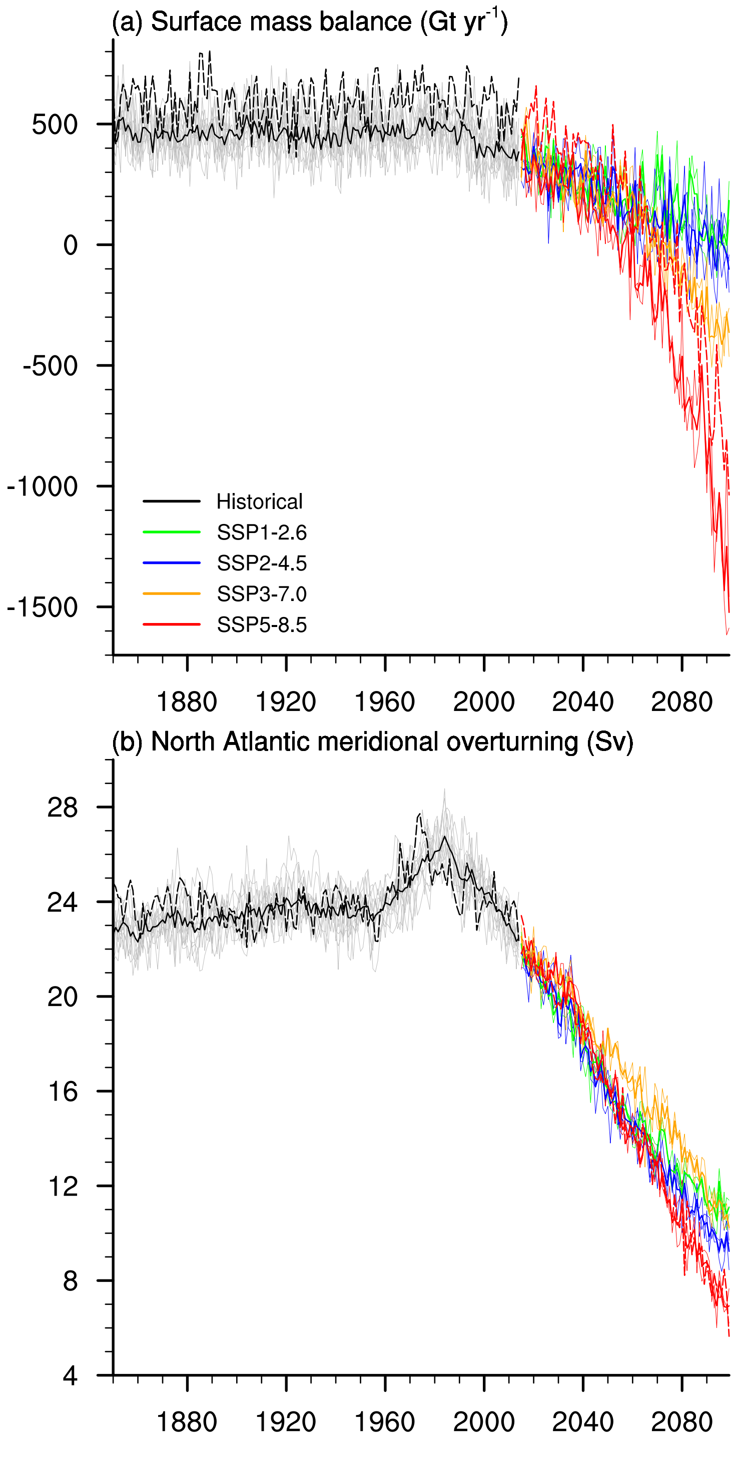

Figure 4. Comparison of a) SMB (Gt yr^{-1}) and b) NAMOC index (Sv) evolution for the historical (black, dashed) and SSP5-8.5 (red, dashed) coupled simulations in this paper versus CESM2.1 historical and scenario simulations with a prescribed-surface-elevation, non-dynamical Greenland ice sheet (that is, with non-active CISM2.1). Thick lines represent scenario-ensemble means.